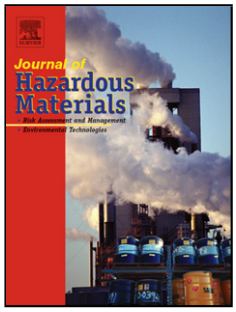

Title: Fluoride adsorption studies on mixed-phase nano iron oxides prepared by surfactant mediation-precipitation technique

Authors: M. Mohapatra, K. Rout, P. Singh, S. Anand, S. Layek, H.C. Verma, B.K. Mishra

PII: S0304-3894(10)01656-0
DOI: doi:10.1016/j.jhazmat.2010.12.076
Reference: HAZMAT 12593

To appear in: *Journal of Hazardous Materials*

Received date: 3-6-2010
Revised date: 22-11-2010
Accepted date: 15-12-2010

Please cite this article as: M. Mohapatra, K. Rout, P. Singh, S. Anand, S. Layek, H.C. Verma, B.K. Mishra, Fluoride adsorption studies on mixed-phase nano iron oxides prepared by surfactant mediation-precipitation technique, *Journal of Hazardous Materials* (2010), doi:10.1016/j.jhazmat.2010.12.076

Fluoride adsorption studies on mixed-phase nano iron oxides prepared by surfactant mediation-precipitation technique

M.Mohapatra*, K.Rout, P. Singh**, S.Anand, S.Layek[#], H.C.Verma[#], B.K.Mishra

Institute of Minerals and Materials Technology, Bhubaneswar 751 013, Orissa, India

** Murdoch University, Perth, Western Australia

[#] Indian Institute of Technology, Kanpur

* Corresponding author, mail Id: mamatamohapatra@yahoo.com
Telephone: +919937563318

Abstract

Mixed nano iron oxides powder containing goethite (α-FeOOH), hematite (α-Fe_2O_3) and ferrihydrite ($Fe_5HO_8 \cdot 4H_2O$) was synthesized through surfactant mediation-precipitation route using cetyltrimethyl ammonium bromide (CTAB). The X-ray diffraction, FTIR, TEM, Mössbauer spectroscopy were employed to characterize the sample. These studies confirmed the nano powder contained 77% goethite, 9% hematite and 14% ferrihydrite. Fluoride adsorption onto the synthesized sample was investigated using batch adsorption method. The experimental parameters chosen for adsorption studies were: pH (3.0 to 10.0), temperature (35 to 55^oC), concentrations of adsorbent (0.5 to 3.0 g/L), adsorbate (10 to 100 mg/L) and some anions. Adsorption of fluoride onto mixed iron oxide was initially very fast followed by a slow adsorption phase. By varying the initial pH in the range of 3.0 to 10.0, maximum adsorption was observed at a pH of 5.75. Presence of either SO_4^{2-} or Cl^- adversely affected adsorption of fluoride in the order $SO_4^{2-} > Cl^-$. The FTIR studies of fluoride loaded adsorbent showed that partly the adsorption on the surface took place at surface hydroxyl sites. Mössbauer studies indicated that the overall absorption had gone down after fluoride adsorption, that implies it has reduced the crystalline bond strength. The relative absorption area of ferrihydrite was marginally increased from 14 to 17%.

Key Words: CTAB; Mössbauer spectroscopy; Adsorption; Thermodynamics; Kinetics; Fluoride

1. Introduction

Fluoride in drinking water is known for having both beneficial as well as detrimental effects on health. Fluoride is considered to be essential for bones and teeth if present in concentrations in the range of 1.0 to 1.5 mg/L [1] but the higher levels of fluoride lead to dental and skeletal fluorosis. Excess fluoride concentrations in water bodies are prevalent all over the world. Removal of fluoride from contaminated water by different techniques such as chemical precipitation, ion exchange, osmosis, reverse osmosis, nanofiltration, Donnan dialysis, etc. has been reported by numerous researchers. Among all, adsorption technique is widely acceptable and many adsorbents have been tested for fluoride removal from contaminated water [2-10]. However, the viability of adsorption techniques is greatly dependent on the development of adsorptive materials and optimization of the performance of adsorbents. Among various adsorbents tested for fluoride removal from aqueous solutions, activated alumina (AA) appears as one of the most studied adsorbents [11-15]. According to USEPA, the best two technologies generally available (BTGAs) for fluoride removal are (1) adsorption on activated alumina and (2) reverse osmosis [16]. However, slow intra-particle diffusion and accumulation of bacteria in the long run, promoted researchers to scan other possible adsorbents. Recently, micro-nanohierarchal web (MiNaHiWe) of carbon fibres has been reported [17] for efficient removal of dissolved fluoride ions in wastewater over the concentration range of 1-50 mg/L. Onyango et al. [18] used Surface-Tailored zeolite for fluoride removal and reported the adsorption capacity 28-41mg/g which is more than most commercial adsorbents. However, the final water quality after defluoridation and costs are two major limitations to motivate the development of new materials

characterized by high adsorption capacity for fluoride. Both bulk and nano sized Fe_2O_3 and FeOOH in different forms make a category of their own as adsorbents. Zhang et al., [19-20] have reported a Ce–Fe bimetal oxide adsorbent, which showed high adsorption capacity for anions like arsenate, phosphate and fluoride. In another study rare earth based inorganic adsorbents showed good fluoride uptake but the optimum pH was as low as 3.0 [21]. The efficiency of fluoride adsorption depends on the chemical composition and physicochemical characteristics of adsorbent such as shape, size and dispersion of particles. Surfactant assisted precipitation route is one where both dispersion and size of the particles can be tailored. Cetyltrimethyl ammonium bromide (CTAB), a cationic surfactant has shown promise in the synthesis of nano rods/particles with homogeneous size and shape. In the present study an attempt has been made to synthesize nano powders of mixed iron oxide/oxy-hydroxide through surfactant (CTAB) mediation–precipitation technique for developing an efficient adsorbent for fluoride mitigation from aqueous solutions.

2. Experimental procedure

2.1 Materials

$Fe(NO_3)_3.7H_2O$ and cetyltrimethyl ammonium bromide (CTAB) used for synthesis were of Analytical Grade (E Merck, India). Sodium fluoride (Ranchem, India) was used for the preparation of the standard fluoride (1000 mg/L) stock solution. Sodium 2-(para sulfophenyl azo)-1,8-dihydroxy-3,6-naphthalene disulfonate (SPADNS) and zirconyl oxychloride used for fluoride analysis were of GR (E. Merck) grade.

2.2 Preparation of mixed iron oxide/hydroxide sample by surfactant mediation-precipitation technique

100 mL of a 0.88 M $Fe(NO_3)_3$ was taken in a clean, dry beaker. To this 5 mL of 10 % cetyltrimethyl ammonium bromide (CTAB) solution was added and the solution was stirred for 2 h. The pH of the solution was adjusted to 10.0 by addition of 1 M NaOH solution under stirring. The contents were further stirred for 24 h after pH adjustment. The precipitate formed was filtered through a G4 frit crucible and was thoroughly washed with water until the filtrate was free of nitrate. The precipitate was then transferred to a beaker and the volume made up to 500 mL with water. The beaker was kept at 60^0C for 12 h in an oven. After aging, the solution was finally filtered through a G4 crucible, washed thoroughly with water and dried in an oven at 100^0C for 24 h.

2.3. Batch fluoride sorption experiments on the prepared sample and fluoride analysis

A 100 mg/L fluoride stock solution was prepared by dissolving 0.221g of NaF in 1L of double distilled water. The experimental solutions were prepared by appropriate dilutions of the above solution. 0.1 g of the sample was taken in a 100 mL polyethylene plastic vial and 50 mL of fluoride solution of known concentration was added. The contents were kept for constant shaking in a temperature controlled water bath shaker over a period of time and the solids were separated by filtration using 0.45μM filter paper. The solutions were collected for analysis and fluoride concentration in the solutions was determined. Fluoride analysis was carried out by following SPADNS method [22] and the color absorbance was measured on UV/Visible Spectrophotometer.

2.4 Chemical analysis and characterization

The samples were acid digested and iron analysis was done both volumetrically [23] as well as by atomic adsorption spectrophotometer ((Perkin-Elmer Model AA200)).

pH_{PZC} of the synthetic material was determined following Blisterry and Murray method [24]. Accordingly, to a series of well-stoppered 125 mL polyethylene bottles containing 40 mL of 0.01 M KNO_3 electrolyte solution, different volumes of either 0.1 M HCl or 0.1 M NaOH solution were added to obtain wide-ranging pH values from 1.0 to 10.0. The total volume of solution in each bottle was made up to 50 mL by addition of distilled water. After 2 h of equilibration the pH values (pH_i) were noted and 0.2 g of sample was added. After 72 h of equilibration at room temperature with intermittent shaking, the pH value of the supernatant liquid in each bottle was noted (pH_f). The difference between pH_i and pH_f (ΔpH) were then plotted against pH_i, the solution pH at which ΔpH=0 is "the pH_{pzc}" of the sample. The crystal structures of the resulting products were characterized by X-ray diffractometer (Model PW1830 XRD with CoKa radiation, l ¼ 1.79A˚). The FTIR spectra were taken using a JASCO Model 5300 spectrometer in a KBr matrix in the range of 400–4000 cm^{-1}. Transmission Electron Microscopy (TEM) of the typical sample was studied using electron microscope (FEI Technai^{G2} 20 TWIN TEM). A pH-meter (Model: LI-127, ELICO India) was used for pH measurements. UV-VIS spectrophotometer (Model 2101, Shimadzu) was used for fluoride determination.

3. Results and Discussion

3.1 Chemical analysis and characterization

3.1.1 Chemical analysis

The chemical analysis of the sample showed 60.13 % iron content. If the sample was pure FeOOH, its iron content should be 62.8 % and likewise if the sample was hematite (Fe_2O_3), its iron content should have been 69.9 %. The fact that the percentage of iron is lower than both suggest that there should be a third phase with less iron content. Based on the chemical formula ($Fe_5HO_8{\cdot}4H_2O$) for ferrihydrite the theoretical value for

Fe should be 58.1%, hence it is expected that the synthesized sample may be containing ferrihydrite along with other phases of iron. The BET surface area of the sample was estimated to be 201.87 m^2/g.

3.1.2 XRD studies

The XRD pattern of the sample given in Fig.1, shows characteristic strong peaks at 2θ values of 24.68, 42.78, 46.73 and 62.68 corresponding to the major (110), (111) (112) and (122) planes of goethite (JCPDS file Card, No. 03-0249). The peaks corresponding to 2θ values of 38.80 and 42.14 confirm the presence of hematite (JCPDS file Card, No. 33-0664). The peaks at 2θ values of 42.14, 48.17, 53.02, 55.45 correspond to the (110), (200), (113) and (114) planes of the six line ferrihydrite (JCPDS Card No 29-0712). It is clear that the sample is a mixture of goethite, hematite and ferrihydrite.

3.1.3 TEM studies

The sample was sonicated in ethyl alcohol and its TEM image was taken at various magnifications. A typical TEM image given in Fig.2 clearly shows two types of particles. The first type are needle shaped goethite particles having length varying from 50 to 200 nm with breadth of 10 nm. The second type of particles are clusters of agglomerated spherical particles of very fine size. These particles are hematite mixed with ferrihydrite.

3.1.4 Mössbauer spectra of as prepared mixed iron oxide sample

Mössbauer spectrum of the as prepared mixed oxide sample recorded at room temperature is shown in Fig.3a. To get a good fit, shown by the solid line, a total of eight sextet and a doublet were fitted. The values of the fields and the corresponding absorption area are shown in Fig.3b. The sextet at 51.1 T clearly corresponds to hematite

phase. All other sextets ranging from 38T downwards correspond to goethite. The distribution comes because of the structure of the particles as shown in TEM. The goethite particles are in the shape of nano rods with diameter around 10 nm and varying lengths. The nano size results in reduction of hyperfine field due to rapid relaxation of magnetic moments. A distribution in shape and size will correspond to a distribution in the hyperfine field as observed in the spectrum. There is no distribution of B_{hf} around 51T showing that hematite particles are bigger in size and relaxation is not effective. Apart from the six-line components, a doublet with isomer shift 0.25 mm/s with respect to iron and quadruple splitting 0.65 mm/s is also fitted. These parameters match with ferrihydrite and support the XRD interpretation. The relative absorption areas of hematite, goethite and ferrihydrite are 9, 77 and 14% , respectively.

3.2. Adsorption of fluoride on nano mixed iron oxide sample

3.2.1 Effect of pH

The effect of pH on fluoride removal was studied in the range of 3.0 to 10.0 and the results are shown in Fig.4. Other conditions maintained were: time **8 h**, temperature 35^{o}C and adsorbent concentration 1 g/L. Analysis of soluble iron in filtrate after adsorption showed only 0.5 mg/L of iron at a pH of 3 and above this pH no iron dissolution took place. Therefore, the loss of sorbent through dissolution was almost nil during the experiments. As the initial solution pH (pHi) increased from 3.0 to 5.75 percentage of fluoride adsorption increased from 46.51 to 67 %. A decrease in fluoride adsorption from 67 % to 32.42 % was observed with the increase in initial pH from 5.75 to 10.0. Maximum fluoride adsorption was observed at a pH of **5.75.** The fluoride adsorption may be due to the combined effect of both chemical and electrostatic interaction between the oxide surface and fluoride ion and also availability of active sites

on the oxide surfaces. Similar observations of formation of maxima in acidic pH range have been widely reported [25-28]. As reported earlier, anion adsorption on metal oxide surface is through columbic forces and/or ligand exchange reactions, where the anions displace OH− or H_2O from the surface [25]. In our studies it was observed that the pH of the equilibrated solution slightly increased in acidic pH range, while it slightly decreased when the initial solution was alkaline. Hence, the fluoride adsorption on mixed ion oxide may be due to anion exchange at acidic pH and by van der Waals forces at alkaline pH ranges. The most probable mechanism for fluoride adsorption in acidic condition is mainly as [26]:

$$\equiv MOH + H_2O + F^- \rightarrow \equiv MOH_2^+ + F^- + OH^-$$
$$\rightarrow MOH_2 - F + OH^- \rightarrow MF + H_2O + OH^- \quad (1)$$

In the basic condition,

$$MOH + H_2O + X^+ \rightarrow MO^- + H_3O^+ + X^+$$
$$\rightarrow MOX + H_2O + OH^+ \quad (2)$$

where X represents the cation Na^+

Hiemstra and Riemsdijk [29] also reported adsorption of F^- on goethite to be through singly coordinated FeOH groups. At pH > 6.95, the zeta potentials will be negative resulting in repelling the fluoride ions via columbic repulsion. Further at high pH values OH^- ions would compete with F^- ions for adsorption [15, 30-31].

3.2.2. Effect of contact time

Fig.6 shows that the % F^- adsorption increased from 17.18 to 66.0 % as the time increaseed from 15 min to 480 min. Equilibrium was achieved at 420 minutes (seven hours). The fluoride adsorption was initially fast up to 120 min, and then it became slow. The initial rapid adsorption was presumably due to ion exchange with surface hydroxyl

ions of the adsorbent. The slow adsorption in the later stage represents a gradual uptake of fluoride at the inner surface [27]. The fluoride uptake stabilized after a period of 420 minutes. However, to ensure achievement of equilibrium, for rest of the experiments the contact time was maintained as 8 hours.

3.2.3. Effect of adsorbent dose

The effect of adsorbent dosage on fluoride removal at fixed pH and initial fluoride concentration (30 mg/L) under equilibrium condition is shown in Fig.7. It is evident that the percent of fluoride removal increased with the increase of the adsorbent concentration which is due to the fact that a greater amount of adsorbent provides greater number of available binding sites. The decrease in loading capacity is expected as for the same initial concentration of F^- the amount of adsorbent increased.

3.2.4 Effect of initial fluoride concentration

The fluoride concentration was varied from 10 to 100 mg/L while the pH, time, and adsorbent concentration were kept at 5.0, 8 h, and 1 g/L, respectively. The adsorption results are shown in Fig. 8. The maximum loading capacity of 39.4 mg/g was observed till initial F^- concentration of 80 mg/L and on further increase in initial F^- concentration to 100 mg/L, only marginal increase in loading capacity was observed (40.5 mg/g).

Isotherm analysis

The isotherm experiments shown in Fig.8 were fitted to the Langmuir and Freundlich models. The linearised form of the Langmuir (Eq. 1) and Freundlich isotherm (Eq. 2) are given below:

$$\frac{C_e}{q_e} = \frac{1}{Q_o b} + \frac{C_e}{Q_o} \quad (1)$$

$$\log q_e = \log K_F + \frac{1}{n} \log C_e \quad (2)$$

where C_e is equilibrium concentration (mg/L), q_e is the amount adsorbed at equilibrium (mg/g), Q_o is sorption capacity for Langmuir isotherms and '*b*' is an energy term which varies as a function of surface coverage strictly due to variations in the heat of adsorption $1/n$ and K_F are isotherm constants for Freundlich plots. The Langmuir and Freundlich isotherms are shown in Figs. 9 and 10, respectively.

The value of the Langmuir equilibrium coefficient, '*b*', was found to be 0.06 L/g for F^- adsorption with the correlation coefficient value of 0.99. The Langmuir monolayer capacity value was estimated to be 53.19 mg/g. The Freundlich isotherm gave the correlation coefficient value of 0.94. The Freundlich parameters 'K_F' and '*n'* were estimated to be 5.063 and 1.807, respectively. Based on the values of correlation coefficient , Langmuir model was better fitted to the experimental data.

3.2.5. Effect of temperature and thermodynamic feasibility of the process

To study the effect of temperature on adsorption, temperature was varied from 35 to 55^{o}C while keeping the contact time as 8 h. The data shown in Fig.11 reveals that rise in solution temperature has an adverse effect on fluoride adsorption as with the increase in temperature from 35 to 55^{o}C, % F^- adsorption decreased from 67.0 to 6.9%.

The thermodynamic feasibility of the process in the present fluoride-iron oxide system was evaluated from the free energy change following Eq.(3) where ΔG^0 is the

change in free energy, T is the absolute temperature, R is the universal gas constant, and K_c is the equilibrium constant at temperature T ($K_c = C_a/C_e$,where C_e the equilibrium concentration in solution in mg/L and C_a is the adsorbed amount of adsorbate at equilibrium in mg/L). The values of the enthalpy change (ΔH^0) and the entropy change (ΔS^0) of the process were obtained using the van't Hoff equation (Eq.4).

$$\Delta G^0 = -2.303RT \log K_c \quad (3)$$

$$\log K_c = \Delta S^0/ 2.303R - (\Delta H^0/2.303R)1/T \quad (4)$$

ΔG^0 values were estimated as -1.81, -0.618, 3.556 and 7.33 kJ/mole at 35, 40, 45 and 55^{o}C, respectively. These results indicate the feasibility of the process at lower temperature. The van's Hoff plot is shown in Fig.12. From the slope and intercept values of ΔH^0 and ΔS^0 were estimated to be – 94.67 kJ/mole and -300.84 J/mole/deg, respectively. The negative ΔH^0 value confirms the adsorption process to be exothermic in nature while the negative ΔS^0 is indicative of decreased randomness at the solid solution interface during adsorption [32].

3.2.6 . Effects of coexisting anions

The effect of coexisting anions namely sulfate and chloride on fluoride adsorption onto the synthesized sample was examined and the results are given in Fig.13. Sulfate and chloride interfere with fluoride removal even at a concentration of 5 mg/L. However the effect of sulphate is more pronounced than that of chloride. Similar effect has been reported earlier when HFO was taken as an adsorbent [33]. Cl^- had less impact on fluoride adsorption, as Cl^- forms an outer-sphere surface complexes, while SO_4^{2-} forms

both outer-sphere and inner-sphere surface complexes [34]. Therefore, the expected impact of Cl^- on fluoride adsorption is less significant than that of SO_4^{2-}.

4.4. Treatment of ground water

The study has shown that the synthesized mixed iron oxide has a good fluoride adsorption capability. Studies were carried out to remove fluoride from water samples collected from paddy fields at Atri (Khurda, Bhubaneswar, Orissa) hot spring containing 10.25 mg/L fluoride. The pH of this contaminated water was 7.75. The chemical analysis of the water sample showed it to contain 9.6, 11.2, 269.7 and 148.9 mg/L of Ca, Mg, Cl^- and SO_4^{2-}, respectively. The experiments were carried out following stage wise removal of fluoride. The fluoride depleted solution of first stage was contacted with fresh adsorbent for the second stage and so on so forth in next stages. Fig.14 shows that by using 1.5g/L of adsorbent and keeping the contact time as 8 hours, in two stages the fluoride content could be brought to 1.46 mg/L.

4.5. Characterization of fluoride loaded mixed iron oxide sample

4.5.1 XRD studies

The XRD pattern of fluoride loaded sample prepared under the conditions adsorbent dose 1g/L, initial fluoride concentration 100 mg/L, temperature 35^oC and pH 5.75 showed similar pattern as obtained for the as such prepared sample (Fig.1). The XRD data given in Table 1 shows +ve or –ve shifts in peaks corresponding to various phases. The major shifts were observed for the d-values at 4.9736 and 2.454 Å corresponding to goethite phase and at 2.194 Å corresponding to both goethite and

ferrihydrite phases. The 100% RI peak for goethite in the fluoride loaded sample was observed at 2.489 Å which could be due to this being common for goethite and ferrihydrite. From the intensities of various peaks it can also be observed that the adsorption of fluoride in general enhanced the peak intensity of ferrihydrite phase except for the peak appearing at 1.924 Å. These results do indicate goethite and ferrihydrite phases to be providing active sites for adsorption.

4.5.2 FTIR studies

The FTIR spectra of the adsorbent before and after fluoride adsorption are shown in Fig.15. The adsorption bands at 3150-3100, 1635, and 1161cm^{-1} are assigned to the hydroxyl stretching vibration of water, bending mode of water, and the bending vibration of the surface hydroxyl group [35], respectively. The characteristic sharp bands at 799 cm^{-1} and 898 cm^{-1} can be assigned to the Fe−O−H bending vibration of goethite. The 625 cm^{-1} and 470 cm^{-1} band are ascribed to Fe−O stretching vibrations of goethite lattice [36]. This band is affected by the shape of the goethite particles [35, 36]. Fig.15 shows that the band at 1161 cm^{-1} present before adsorption disappeared after fluoride adsorption. It can be deduced that the disappearance of this band is due to the fact that partly adsorption of fluoride has taken place at the hydroxyl site. Because -OH and F^- have nearly the same size, these can exchange for each other and F^- can get adsorbed.

4.5.3 Mössbauer studies

The Mössbauer spectrum of fluoride loaded sample recorded at room temperature is given in Fig.16a and the distribution of B_{hf} and absorption areas in Fig. 16b. One can observe that the overall absorption has gone down as compared to the as- prepared mixed oxide sample. This means that the chemical process during the fluoride adsorption has

reduced the crystalline bond strength. The relative absorption area of ferrihydrite is marginally increased from 14 to 17% with a corresponding small decrease in goethite and hematite absorption areas. Adsorption at the surface has largely retained the Mössbauer parameters like B_{hf} and IS.

5. Conclusions

Nano ranged mixed iron oxide sample was prepared following surfactant mediation- precipitation technique. The instrumental analysis which included XRD, FTIR, TEM and Mossbauer spectroscopy confirmed the sample to be a mixture of goethite, hematite and ferrihydrite. The surface area of the prepared sample was 201.87 m^2/g. Fluoride adsorption studies were carried by varying time, pH, amount of adsorbent and adsorbate. Results showed that the fluoride adsorption was maximum at a pH of 5.75, then decreased with further increase of pH. From the thermodynamic studies it can be concluded that the fluoride adsorption on nano mixed iron oxides is thermodynamically favorable at low temperatures, and is exothermic in nature. Major co-existing anions adversely affected fluoride adsorption according to their affinity on the surface in the following order: $SO_4^{2-} > Cl^-$. The results obtained on XRD, FTIR and Mossbauer studies on the loaded adsorbent have been discussed.

Acknowledgements

The authors are thankful to Prof. B.K. Mishra, Director, Institute of Minerals and Materials Technology (IIMT), Bhubaneswar, for his kind permission to publish this work. The authors are thankful to Dr. Debadhyan Behera for carrying out TEM and EDAX analysis.

References

[1] WHO (World Health Organization), Guidelines for Drinking Water Quality, World Health Organization, Geneva, 2004.

[2] A.A.M. Daifullah, S.M. Yakout, S.A. Elreefy, Adsorption of fluoride in aqueous solutions using $KMnO_4$-modified activated carbon derived from steam pyrolysis of rice straw, J. Hazard. Mater. 147 (2007) 633–643.

[3] M.M. Shihabudheen, K.S. Atul, P. Ligy, Manganese-oxide-coated alumina: a promising sorbent for defluoridation of water, Water Res. 40 (2006) 3497–3506.

[4] R. Aldaco, A. Garea, A. Irabien, Calcium fluoride recovery from fluoride wastewater in a fluidized bed reactor, Water Res. 41 (2007) 810–818.

[5] E. Akbar, S.O. Maurice, O. Aoyi, A. Shigeo, Removal of fluoride ions from aqueous solution at low pH using schwertmannite, J. Hazard. Mater. 152 (2008) 571–579.

[6] S. Meenakshi, N. Viswanathan, Identification of selective ion-exchange resin for fluoride sorption, J. Colloid Interface Sci. 308 (2007) 438–450.

[7] A. Tor, Removal of fluoride from water using anion-exchange membrane under Donnan dialysis condition, J. Hazard. Mater. 141 (2007) 814–818.

[8] S. Lahnid, M. Tahaikt, K. Elaroui, I. Idrissi, M. Hafsi, I. Laaziz, Z. Amor, F. Tiyal, A. Elmidaoui, Economic evaluation of fluoride removal by electrodialysis, Desalination 230 (2008) 213–219.

[9] J. Liu, Z. Xu, X. Li, Y. Zhang, Y. Zhou, Z. Wang, X. Wang, An improved process to prepare high separation performance PA/PVDF hollow fiber composite nanofiltration membranes, Sep. Purif. Technol. 58 (2007) 53–60.

[10] P. Sehn, Fluoride removal with extra low energy reverse osmosis membranes: three years of large scale field experience in Finland, Desalination 223 (2008) 73–84.

[11] S. Ayoob, A. K. Gupta, Insights into isotherm making in the sorptiove removal of fluoride from drinking water, J. Hazard. Mater. 152 (2008) 976-985.

[12] V.S. Chauhan, P.K.Dwivedi, L. Iyengar, Investigations on activated alumina based domestic defluoridation units, J. Hazard. Mater. 139 (2007) 103–107.

[13] S. Ghorai, K.K. Pant, Investigations on the column performance of fluoride adsorption by activated alumina in a fixed-bed, Chem. Eng. J. 98 (2004) 165–173.

[14] N. Das, P. Pattanik, R. Das, Defluoridation of drinking water using activated titanium rich bauxite, J. Coll. Interf. Sci. 292 (2005) 1–10.

[15] H. Lounici, L. Addour, D. Belhocine, H. Grib, S. Naicolas, B. Bariou, N. Mameri, Study of a new technique for fluoride removal from water, Desalination 114 (1997) 241–251.

[16] US EPA, Water Treatment Technology Feasibility Support Document for Chemical Contaminants; In Support of EPA Six-Year Review of National Primary DrinkingWater Regulations. EPA 815-R-03-004, 2003.

[17] A. K. Gupta, D. Deva, A. Sharma, Nishith Verma, Adsorptive removal of fluoride by micro-nanohierarchal web of activated carbon fibers, Ind. Eng. Chem. Res. 48 (2009) 9697–9707.

[18] M. S. Onyango, T. Y.Leswif, A. Ochieng, D. Kuchar, F. O. Otieno, H. Matsuda, Breakthrough analysis for water defluoridation using Surface-Tailored Zeolite in a fixed bed column, Ind. Eng. Chem. Res. 48(2) (2009) 931-937.

[19] Y. Zhang, M. Yang, X. Huang, Arsenic(V) removal with a Ce(IV)-doped iron oxide adsorbent, Chemosphere 51 (2003) 945–952.

[20] Y. Zhang, M. Yang, X.M. Dou, H. He and D.S. Wang, Arsenate adsorption on an Fe–Ce bimetal oxide adsorbent: role of surface properties, Environ. Sci. Technol. 39 (2005) 7246–7253.

[21] Z.Z. Jiao, Y. Zhang, M. Yang, X. Huang, K.M. Ma, Removal of fluoride using rare earth based-inorganic adsorbent, Environ. Chem. Chinese 21 (2002) 365–370.

[22] A. E. Reenberg, L.S. Coesreri, A. D. Eaton, Standard Methods For the Examination of Water and Waste Water . John Willey and Sons, New York, 1987, p.325.

[23] A.I. Vogel, A Text Book of Quantitative Inorganic Analysis, English Language Book Society and Longmans Green Publishers, London (2000).

[24] L.S. Balistrieri , J.W. Murray, The surface chemistry of goethite α-FeOOH in major ion seawater. Am. J. Sci. 281 (1981) 788–806.

[25] Y. Wang, E.J.Reardon, Activation and regeneration of a soil sorbent for defluoridation of drinking water. Applied Geochemistry, 16(2001) 531-539.

[26] M. G. Sujana, S. Anand, Iron and aluminium based mixed hydroxides: A novel sorbent for fluoride removal from aqueous solutions. Applied Surface Science 256 (2010) 6956–6962.

[27] M.G. Sujana, H.K Pradhan, S. Anand, Studies on sorption potential of some geomaterials for fluoride removal from aqueous solutions, J. Hazar. Mater. 161(I) (2009) 120-125.

[28] M.G.Sujana, G.Soma, N.Vasumathi, S.Anand, Studies on fluoride adsorption capacities of amorphous Fe/Al mixed hydroxides oxides from aqueous solutions. J. Fluorine Chem. 130(8) (2009)749-754.

[29] T. Hiemstra, W.H.V. Riemsdijk, Fluoride adsorption on goethite in relation to different types of surface sites. J. Colloid Interf. Sci.225(1) (2000) 94-104.

[30] A.L. Valdivieso, J.L. Reyes Bahena, S. Song, R. Herrera Urbina, Temperature effect on the zeta potential and fluoride adsorption at the α-Al_2O_3/aqueous solution interface, J. Colloid Interf. Sci. 298 (2006) 1–5.

[31] R. L. Ramos**,** J. O-Turrubiartes**,** M.A. Sanchez-Castillo, Adsorption of fluoride from aqueous solution on aluminum-impregnated carbon, Carbon 37 (1999) 609–617.

[32] D.B. Singh, G. Prasad, D.C. Rupainwar, Adsorption technique for the treatment of As(V)-rich effluents, Colloid Surf. A: Physicochem. Eng. Aspects 111 (1996) 49–56.

[33] Y. Tang, X, Guan, J. Wang, N. Gao, M.R. McPhail, C.C. Chusuei, Fluoride adsorption onto granular ferric hydroxide: Effects of ionic strength, pH, surface loading, and major co-existing anions. J. Hazard. Mater. 171 (2009) 774–779.

[34] A. Tor, Y. Cengeloglu, M.E. Aydin, M. Ersoz, Removal of phenol from aqueous phase by using neutralized red mud. J. Colloid Interf. Sci. 300 (2006) 498–503.

[35] H.D.Ruan, R.I.Frost, J.T.Kloprogge, L. Duong, Infrared spectroscopy of goethite dehydroxylationl: III. FT-IR microscopy of in situ study of the thermal transformation of goethite to hematite. Spectrochimica Acta Part A, 58 (2002) 967–981.

[36] K.M. Parida, J. Das, Studies on ferric oxide hydroxides: II. Structural properties of goethite samples (α-FeOOH) prepared by homogeneous precipitation from $Fe(NO_3)_3$ solution in the presence of sulfate ions. J. Colloid Interf. Sci. 178 (1996) 586–593.

Figure captions

Fig.1. XRD pattern of mixed iron oxide sample. G : goethite, F: Ferrihydrite and H: hematite.

Fig.2. TEM image of mixed iron oxide sample

Fig.3. (a) Mössbauer spectrum of mixed iron oxide sample, recorded at room temperature. (b) B_{hf} and absorption areas of the sextets fitted.

Fig.4. Effect of solution pH on fluoride removal. Conditions: adsorbent dose 1g/L, initial fluoride concentration 30 mg/L, temperature 35^{o}C and contact time 8 h.

Fig.5. pH_{PZC} of the mixed iron oxide sample obtained by solid addition method.

Fig.6. Effect of contact time on fluoride removal. Conditions: adsorbent dose 1 g/L, initial fluoride concentration 30 mg/L, temperature 35^{o}C and pH 5.75.

Fig.7 Effect of adsorbent dose of fluoride removal. Conditions: initial fluoride concentration 30 mg/L, temperature 35^{o}C, pH 5.75 and contact time 8 h.

Fig.8. Effect of initial F^- concentration on its adsorption Conditions: adsorbent dose 1g/L, temperature 35^{o}C, pH 5.75 and contact time 8 h

Fig. 9 Langmuir adsorption isotherm (data corresponding to Fig.8).

Fig.10 Freundlich adsorption isotherm (data corresponding to Fig.8)

Fig.11 Effect of temperature on fluoride removal. Conditions: initial fluoride concentration 30 mg/L, adsorbent dose 1 g/L, pH 5.75 and contact time 8 h.

Fig.12 van't Hoff plot

Fig.13 Effect of chloride and sulphate on % fluoride adsorption on nano mixed iron oxide sample. Condn: initial F^- concn. 30 mg/L, adsorbent dose 1 g/L, temp. 35^{o}C, pH 5.75 and time 2 h.

Fig.14. Stage wise removal of fluoride from contaminated ground water on mixed iron oxide sample. Conditions: Initial F^- concn. 10.25 mg/L, time 8 h, adsorbent dose 1.5g/L in each stage.

Fig.15 Comparison of FTIR pattern of (a) as prepared mixed oxide sample and (b) fluoride loaded sample.

Fig. 16. (a) Mössbauer spectrum of the fluoride loaded mixed oxide sample, recorded at room temperature. (b) B_{hf} and absorption areas of the sextets fitted.

Table 1

As prepared sample d-spacing [Å]	Rel. Int. [%]	F^{-1} loaded sample d-spacing [Å]	Rel. Int. [%]	Shift in d-values
4.97336G	15.98	5.09019	23.84	+0.116
4.18726G	100.00	4.27375	89.11	+ 0.086
3.38095G	10.76	3.44524	26.02	+0.064
2.69442G,H	59.77	2.73334	67.85	+ 0.038
2.58479G,H	29.73	2.61704	45.64	+ 0.032
2.48980G, F	31.57	2.48127	100.00	-0.008
2.45404G	93.77	2.28055	44.87	-0.173
2.25701G,H	25.63	2.21573	49.50	-0.041
2.19333G,F	32.85	2.02928	25.86F	-0.164
1.92402G,F	9.12	1.94047	26.27	+0.016
1.80264G,F	9.17	1.81789	31.65	+ 0.015
1.72083G,H	38.92	1.73432	56.74F	+0.013
1.69448G,H	17.25	1.70985	42.23	+ 0.015

G Goethite; F Ferrihydrite; H Hematite

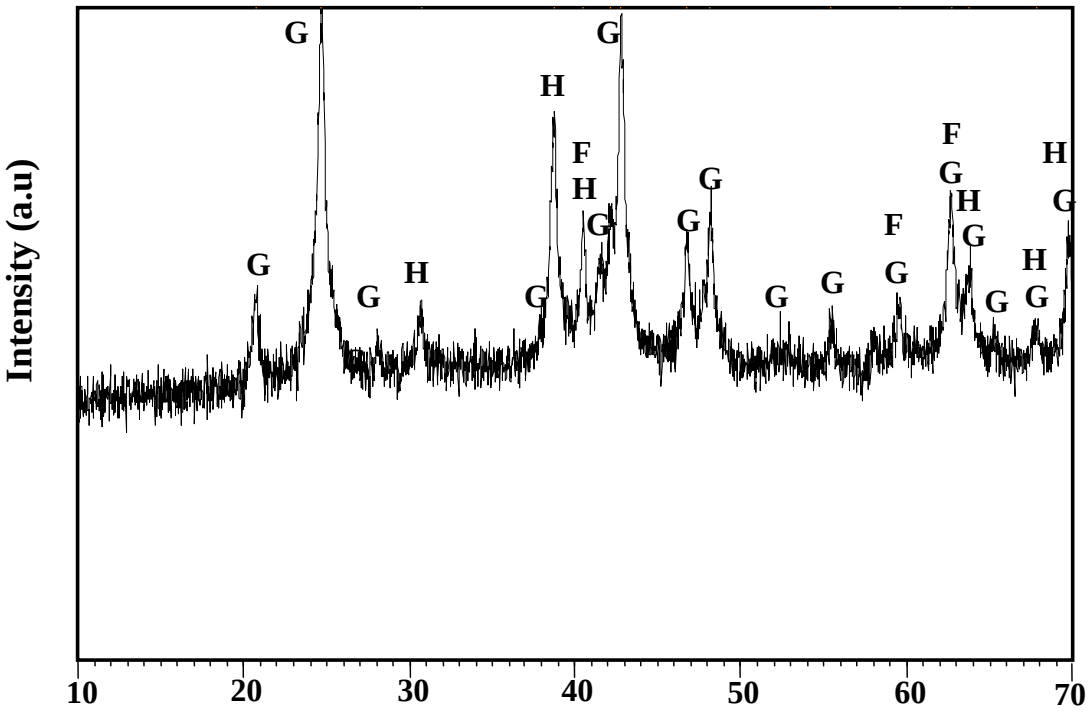

Fig.1. XRD pattern of mixed iron oxide sample. G : goethite, F: Ferrihydrite and H: hematite.

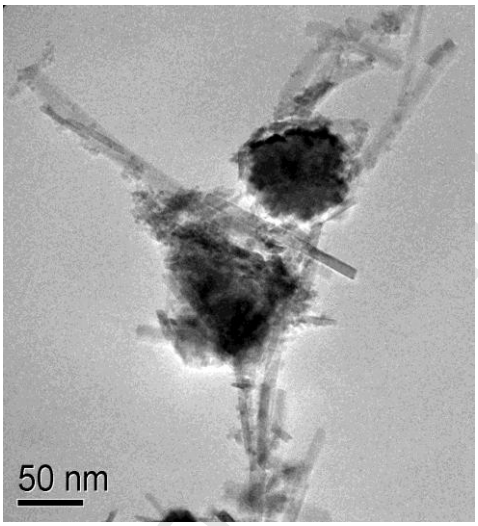

Fig.2. TEM image of mixed iron oxide sample

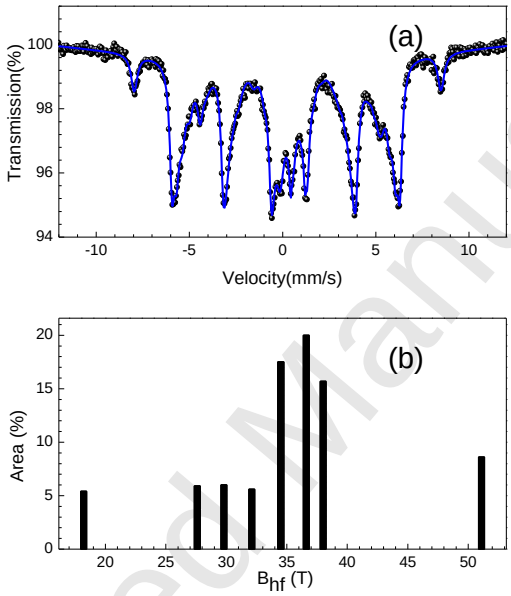

Fig.3. (a) Mössbauer spectrum of mixed iron oxide sample, recorded at room temperature. (b) B_{hf} and absorption areas of the sextets fitted.

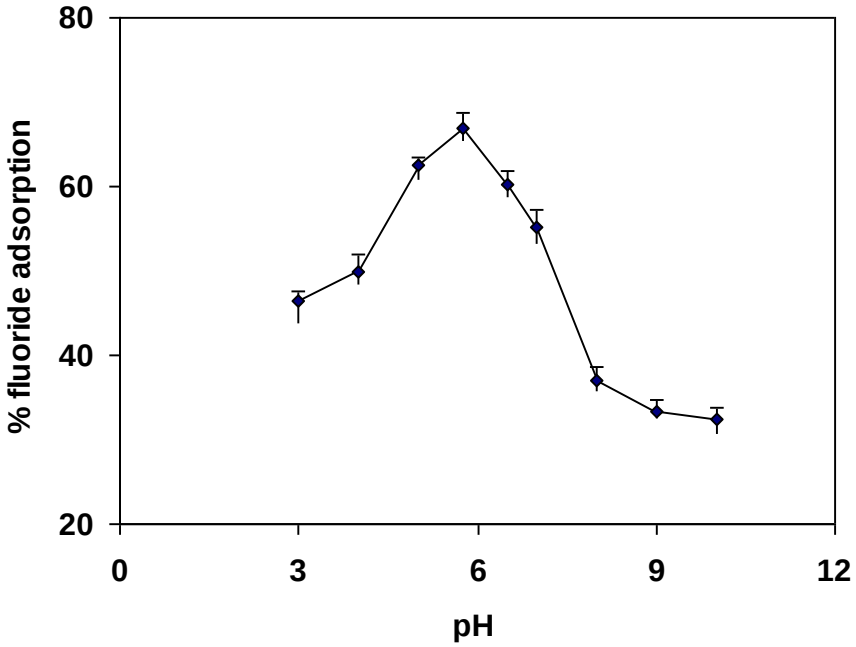

Fig.4. Effect of solution pH on fluoride removal. Conditions: adsorbent dose 1g/L, initial fluoride concentration 30 mg/L, temperature 35^{o}C and contact time 8 h.

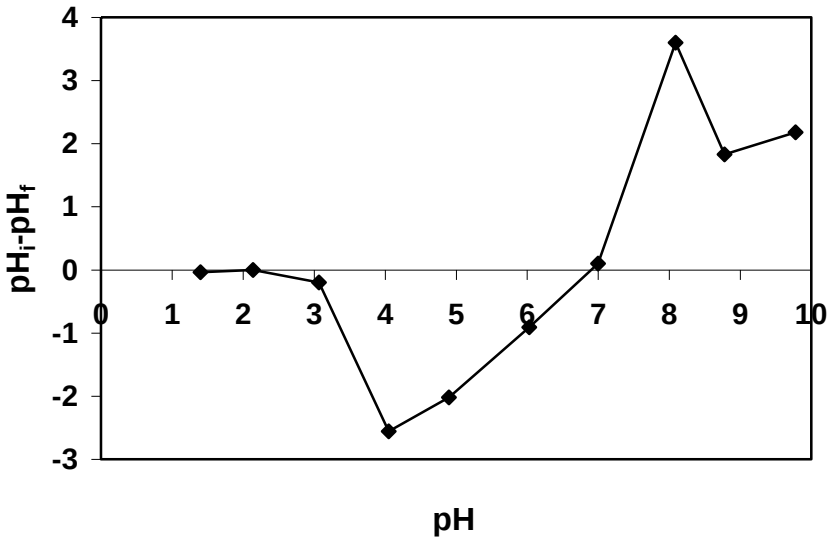

Fig.5. pH_{PZC} of the mixed iron oxide sample obtained by solid addition method.

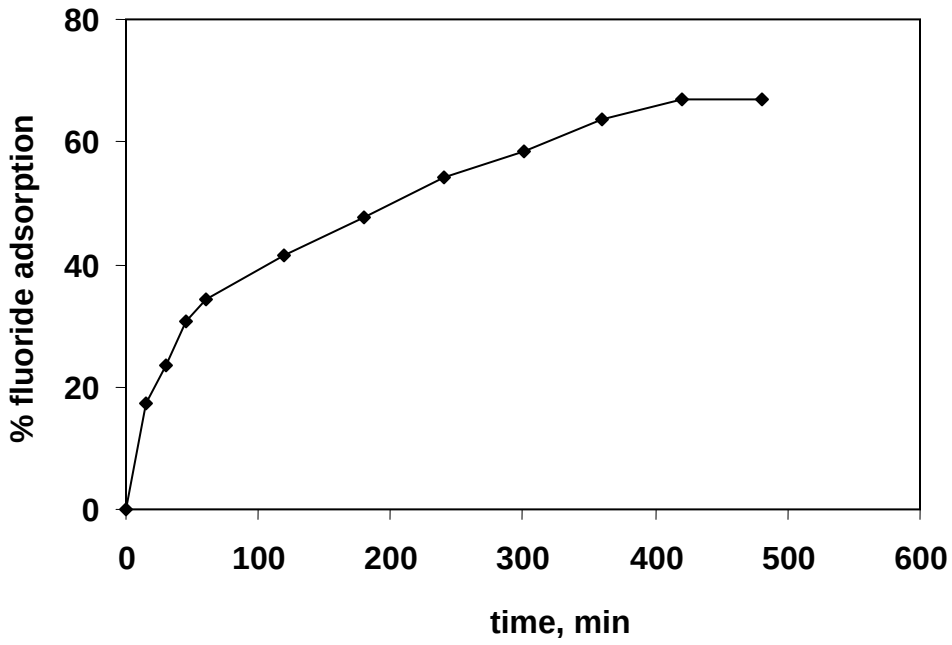

Fig.6. Effect of contact time on fluoride removal. Conditions: adsorbent dose 1 g/L, initial fluoride concentration 30 mg/L, temperature 35^{o}C and pH 5.75.

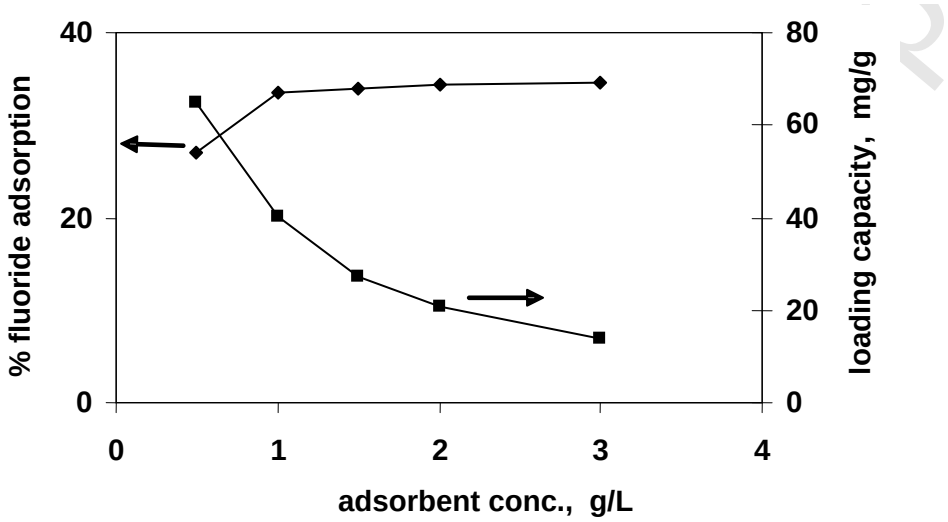

Fig.7 Effect of adsorbent dose of fluoride removal. Conditions: initial fluoride concentration 30 mg/L, temperature 35^{o}C, pH 5.75 and contact time 8 h.

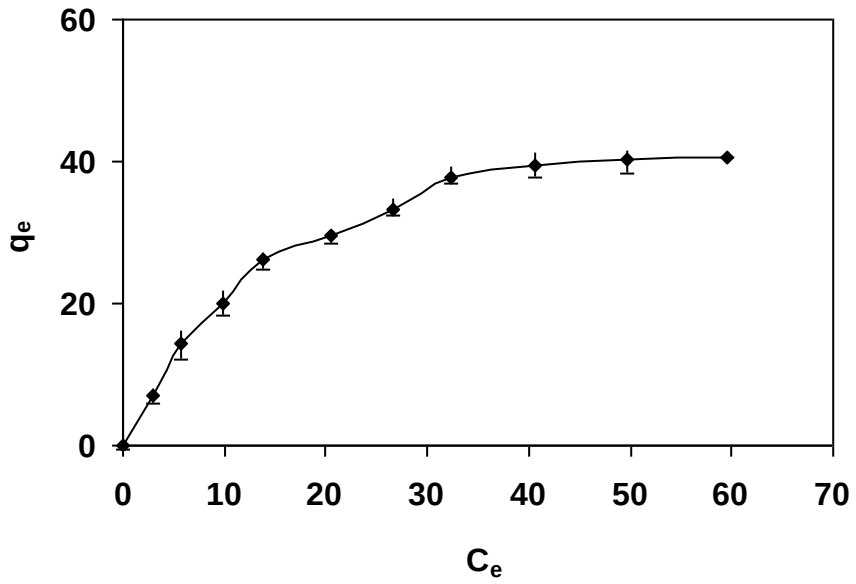

Fig.8. Effect of initial F^- concentration on its adsorption Conditions: adsorbent dose 1g/L, temperature 35^{o}C, pH 5.75 and contact time 8 h

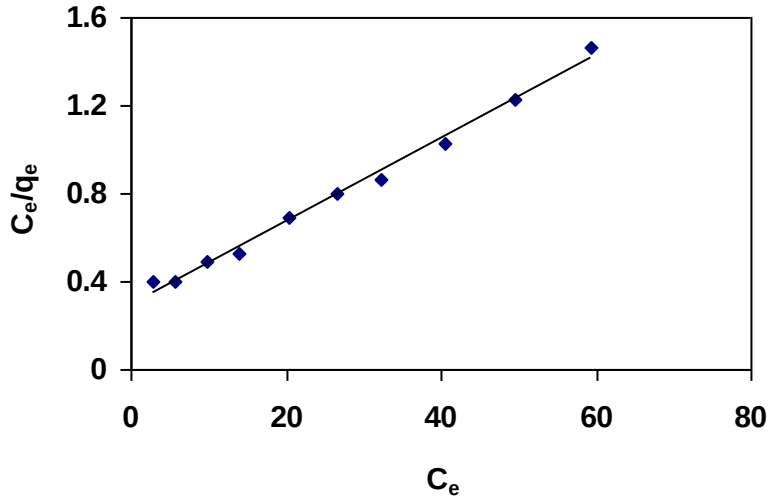

Fig. 9 Langmuir adsorption isotherm (data corresponding to Fig.8).

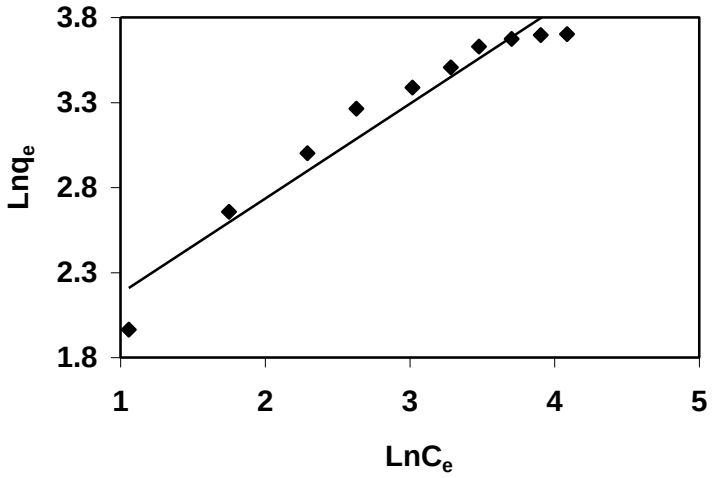

Fig.10 Freundlich adsorption isotherm (data corresponding to Fig.8)

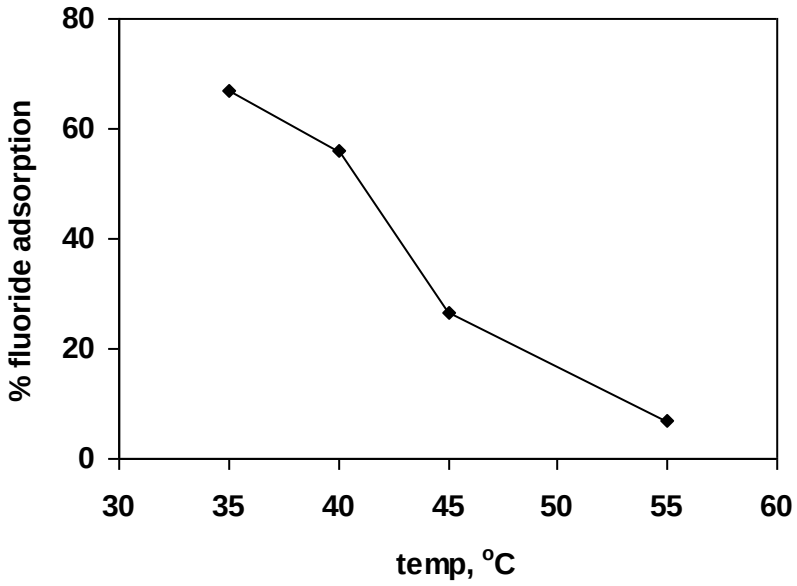

Fig.11 Effect of temperature on fluoride removal. Conditions: initial fluoride concentration 30 mg/L, adsorbent dose 1 g/L, pH 5.75 and contact time 8 h.

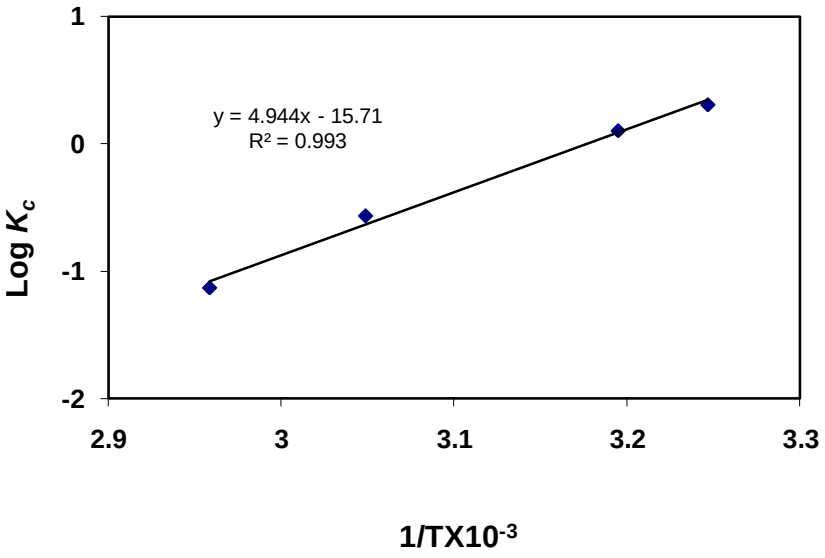

Fig. 12 Van't Hoff plot

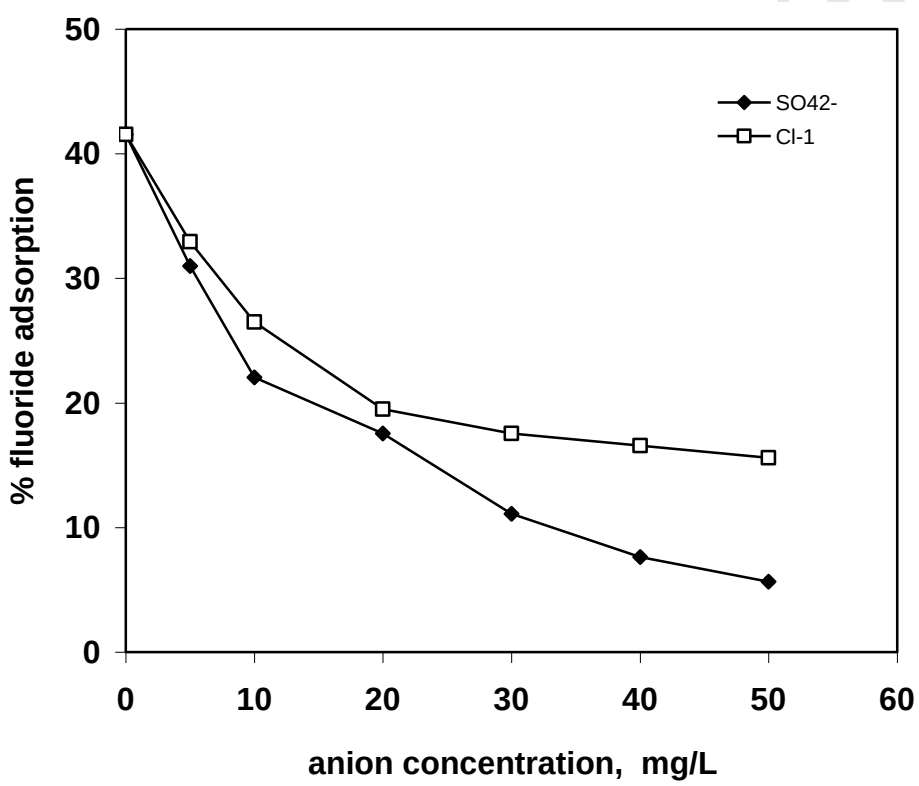

Fig.13 Effect of chloride and sulphate on % fluoride adsorption on nano mixed iron oxide sample. Condn: initial F^- concn. 30 mg/L, adsorbent dose 1 g/L, temp. 35^oC, pH 5.75 and time 2 h.

.

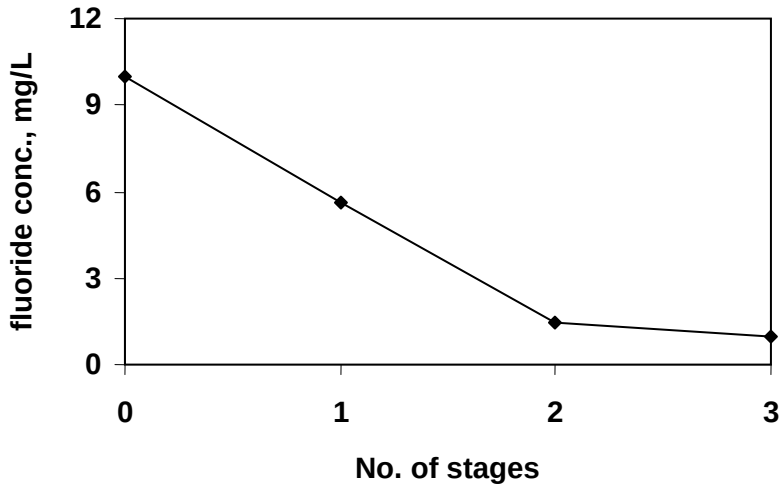

Fig.14. Stage wise removal of fluoride from contaminated ground water on mixed iron oxide sample. Conditions: Initial F^- concn. 10.25 mg/L, time 8 h, adsorbent dose 1.5g/L in each stage.

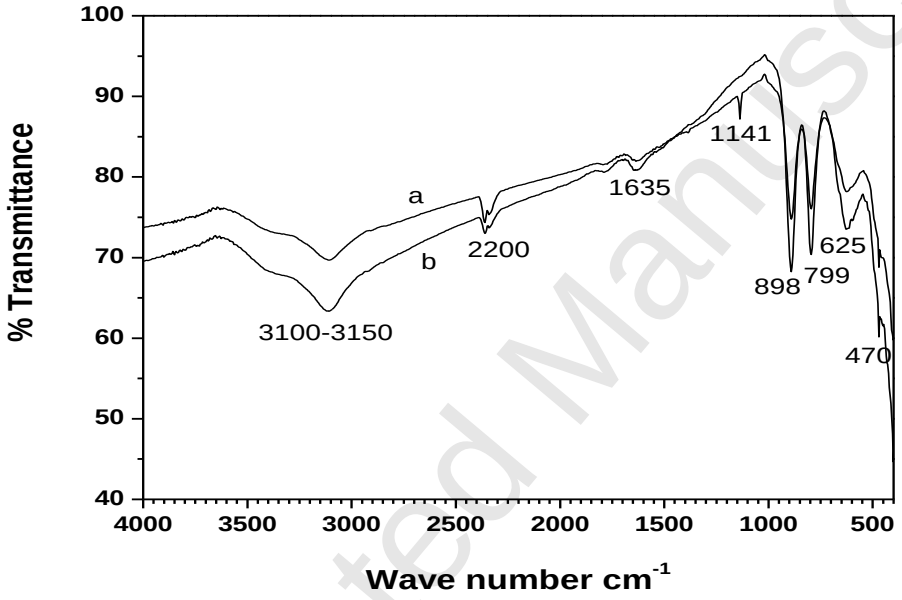

Fig.15 Comparison of FTIR pattern of (a) as prepared mixed oxide sample and (b) fluoride loaded sample.

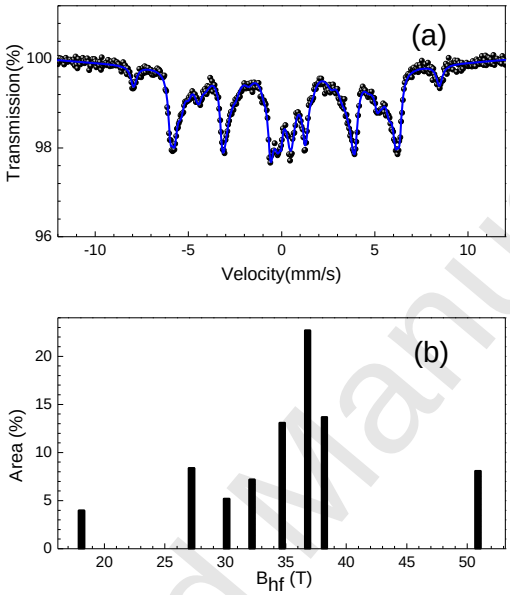

Fig. 16. (a) Mössbauer spectrum of the fluoride loaded mixed oxide sample, recorded at room temperature. (b) B_{hf} and absorption areas of the sextets fitted.